

# A size-resolved model and a four-mode parameterization of dry deposition of atmospheric aerosols

Jian Feng<sup>1</sup>

Received 24 May 2007; revised 10 January 2008; accepted 7 March 2008; published 17 June 2008.

[1] To deposit on the ground surface, an airborne aerosol particle needs to pass through an aerodynamic resistance layer and a quasi-laminar sublayer just adjacent to the surface. Traditionally, it is believed that the main mechanisms through which a particle overcomes the resistance from the quasi-laminar sublayer are Brownian diffusion, interception, inertial impaction, and gravitational settling. In this study, a size-resolved dry deposition model is formulated, which includes a new proposed dry deposition mechanism, the burst effect of eddy turbulence. The effects on dry deposition of particles by Brownian diffusion and inertial impaction are parameterized through the Schmidt number and the Stokes number, respectively. On the basis of the similarity between deposition of particles on walls of pipes and deposition of atmospheric particles on the ground surface, the burst effect of eddy turbulence is parameterized with the roughness Reynolds number. Through the roughness Reynolds number the effect on dry deposition by the surface roughness is parameterized into the model. Since the dry deposition velocity depends on particle size strongly, a four-mode parameterization of dry deposition is proposed for use in atmospheric dispersion models. For each aerosol mode the parameterization of the bulk dry deposition velocity is made up of two terms: the Reynolds term and another term that is a power law function of friction velocity. The dry deposition velocities predicted by the model and the four-mode parameterization are compared with the measurements reported in the literature, and good agreements are achieved.

**Citation:** Feng, J. (2008), A size-resolved model and a four-mode parameterization of dry deposition of atmospheric aerosols, *J. Geophys. Res.*, 113, D12201, doi:10.1029/2007JD009004.

## 1. Introduction

[2] Airborne aerosol particles are brought to the Earth's surface through dry and wet deposition. The relative importance of these two processes depends on meteorological conditions and particle size. Understanding and modeling these two deposition processes are required in air quality monitoring, environmental emergency response, as well as weather and climate studies. In this study, we will focus on the issue of dry deposition.

[3] Dry deposition is usually described by the ratio of the dry deposition flux to the air concentration above the surface. Since this ratio has a unit of meter per second, it is commonly referred to as dry deposition velocity. Studies of dry deposition of atmospheric aerosol particles were carried out in parallel through modeling and field experiments. Reviews of the past studies are given by *Sehmel* [1980], *Ruijgrok et al.* [1995], *Wesely and Hicks* [2000], and *Pryor et al.* [2007]. Generally there are two types of models. The first kind is not size-resolved and predicts bulk dry

deposition velocities which apply to particles over the whole size range [*Wesely et al.*, 1985; *Ruijgrok et al.*, 1997]. The second kind is size-resolved and predicts dry deposition velocities for particles with specific sizes. A number of size-resolved dry deposition models exist. Most of them are only for one or a few specific surfaces [*Schack et al.*, 1985; *Ibrahim et al.*, 1983; *Wiman and Agren*, 1985; *Peters and Eiden*, 1992; *Davidson et al.*, 1982; *Legg and Price*, 1980; *Bache*, 1979; *Slinn*, 1982; *Slinn and Slinn*, 1980; *Williams*, 1982]. Other models can be applied to more surfaces through specifying different parameterizations and coefficients for different surfaces [*Giorgi*, 1986; *Zhang et al.*, 2001; *Nho-Kim et al.*, 2004]. The model of *Sehmel and Hodgson* [1978] is a universal one that can be applied to any surface in that the model parameterizes the surface roughness length as an input parameter. *Slinn's* [1982] model has been widely used [*Ruijgrok et al.*, 1997] and the framework of the model has been adapted in some later developed models [*Zhang et al.*, 2001; *Nho-Kim et al.*, 2004].

[4] Discrepancies between some of these models are quite significant. *Van Aalst* [1986] compared the predictions from 6 dry deposition models. For the same particle size, ground surface and wind friction velocity, the dry deposition

<sup>1</sup>Canadian Meteorological Centre, Meteorological Service of Canada, Dorval, Quebec, Canada.

velocity from one model can be 10–50 times larger than that from another model. Part of these discrepancies is due to the parameterizations of deposition processes, namely diffusion, interception and impaction. Using different mathematical expressions for these processes from some of these models, and the framework of the model of *Slinn* [1982], *Ruijgrok et al.* [1995] obtained considerable differences in dry deposition velocity, especially in the submicron range. Discrepancies between models and measurements are even larger. Several decades after the studies of field measurements and model predictions of the dry deposition of particles, there are still substantial and systemic discrepancies, especially underestimation of dry deposition velocity by models in the size range of  $0.1 \sim 1 \mu\text{m}$  on rough surfaces. A recent process-originated model [*Nho-Kim et al.*, 2004] still underestimated by about a factor of 5 the dry deposition of particles to highly rough surfaces in this size range. This submicron range is particularly important for air quality modeling since a significant percentage of aerosol mass from urban pollution falls into this range. Although part of these discrepancies can be attributed to measurement errors, consistent and significant discrepancies as high as over one order of magnitude imply that some additional deposition mechanism might have been excluded in these process-originated models. This implication was further reinforced by *Wyers and Duyzer* [1997] in measuring dry deposition of sulphate aerosols to coniferous forest. They derived a near-linear relationship between dry deposition velocity and friction velocity for sulphate aerosols, and concluded that an unexplained deposition mechanism, together with the impaction deposition, might be responsible

ization of dry deposition velocity for use in atmospheric dispersion models.

## 2. Development of a New Size-Solved Dry Deposition Model

### 2.1. Modeling of Dry Deposition of Aerosols in the Atmosphere

[6] Modeling of dry deposition in atmospheric models usually adopts the similarity between the dry deposition process and the electrical resistance. A detailed description of the dry deposition resistance model is given by *Seinfeld and Pandis* [2006]. In this resistance model, a particle needs to pass through an aerodynamic resistance layer and a quasi-laminar resistance layer to deposit on a ground surface. An aerodynamic resistance is the resistance that a particle needs to overcome when passing through an atmospheric layer above a ground surface. A quasi-laminar resistance is the one from a very thin viscous layer just adjacent to a ground surface. On the basis of the similarity analysis, the dry deposition velocity can be expressed as

$$V_d = V_t + \frac{1}{r_a + r_s + r_a r_s V_t}, \quad (1)$$

where  $V_t$  and  $r_a$  are the terminal velocity of a particle and aerodynamic resistance respectively;  $r_s$  is the combination of  $r_b$ , the quasi-laminar resistance, and  $r_c$ , the resistance from the ground surface. If we assume a particle will adhere to a ground surface upon contact, the resistance from the surface will be null. The aerodynamic resistance can be expressed as [*Seinfeld and Pandis*, 2006]

$$r_a = \begin{cases} \frac{1}{ku_*} \left[ \ln\left(\frac{z}{z_0}\right) + 4.7(\zeta - \zeta_0) \right] & \text{(stable)} \\ \frac{1}{ku_*} \ln\left(\frac{z}{z_0}\right) & \text{(neutral)} \\ \frac{1}{ku_*} \left[ \ln\left(\frac{z}{z_0}\right) + \ln\left(\frac{(\eta_0^2 + 1)(\eta_0 + 1)^2}{(\eta^2 + 1)(\eta + 1)^2}\right) + 2(\tan^{-1} \eta - \tan^{-1} \eta_0) \right] & \text{(unstable)}, \end{cases} \quad (2)$$

for the derived near-linear relationship. The reason is that if the impaction is the only mechanism, it would suggest the dry deposition velocity has a much stronger dependence on friction velocity than the derived near-linear one [*Van Aalst*, 1986]. This unexplained mechanism couldn't be Brownian diffusion since it is not efficient in this size range.

[5] The discrepancies between the models and the field measurements, and the indication that an unexplained deposition mechanism exists, suggest that a deposition mechanism might have been missing in most previous theoretical and semiempirical dry deposition models. In this study, we develop a new semiempirical size-resolved dry deposition model. A new dry deposition mechanism, the burst effect of atmospheric eddy turbulence, is introduced and included in modeling dry deposition of atmospheric aerosols. We parameterize this eddy turbulence effect through the roughness Reynolds number. Using the new developed model, we will present a four-mode parameter-

where  $\eta = (1 - 15\zeta)^{1/4}$ ,  $\eta_0 = (1 - 15\zeta_0)^{1/4}$ ,  $\zeta = z/L$ , and  $\zeta_0 = z_0/L$ .  $k$  is the von Karman constant with a value  $\sim 0.4$ ;  $u_*$  is the friction velocity;  $z$  is the reference height where the dry deposition velocity is defined;  $z_0$  is the surface roughness length; and  $L$  is the Monin-Obukhov length.

[7] Traditionally it is believed that the main mechanisms through which a particle can pass through a quasi-laminar resistance layer include Brownian diffusion, inertial impaction and gravitational sedimentation. Most of these mechanisms are very size-dependent. Brownian diffusion is very efficient for small particles with diameters from a few nanometers up to  $0.1 \mu\text{m}$ . When a particle's diameter is over a few micrometers, the mass of the particle will make it unable to follow the airflow very well, and collide with the surface of obstacles. Therefore, inertial impaction becomes efficient for a particle with a diameter of greater than a few micrometers. For particles with diameters of over  $10 \mu\text{m}$ , the gravitational settling velocities get more and more significant. In the next subsection, we will present a

deposition mechanism that has been absent in most previous dry deposition models.

## 2.2. Burst Effect of Turbulence

[8] Under most meteorological and ground surface conditions, the atmospheric surface flow is turbulent. Turbulence affects particle deposition through two distinct mechanisms: the turbulence diffusion and the burst effect of turbulence. The later mechanism is often also referred to as turbophoresis in the literature [Caporaloni *et al.*, 1975; Guha, 1997; Young and Leeming, 1997]. In this study, we refer to the second turbulent mechanism as “the burst effect of turbulence” as it is more straightforward. While the turbulence diffusion mechanism is well known to researchers in the field of particle deposition, the burst effect of turbulence, although not a small correction, has just been recognized by very few people [Young and Leeming, 1997]. The burst effect of turbulence refers to the tendency for particles to migrate toward the direction of decreasing turbulence. From observations, it was found that the fluid movement toward the collecting surface occurs through high-speed perturbations, while the fluid movement away from the collecting region is much slower [Kline *et al.*, 1967]. Owen [1969] and Liu and Agarwal [1974] proposed that particles are transported to the deposition surface through high-speed bursts, and that outside the collecting region, the particles are transported through turbulent diffusion. Caporaloni *et al.* [1975] was the first to recognize this phenomenon in theory [Reeks, 1983; Sippola and Nazaroff, 2002]. Similar to the motion of a particle driven by a temperature gradient, which is commonly referred to as thermophoresis, the gradient of turbulence fluctuating velocity (rms of velocity) works in the same way on particles. Since the turbulent vertical velocity fluctuation decays to zero around a boundary surface, the near-surface turbulence is highly inhomogeneous, and particles are driven toward the boundary surface by the gradient of the turbulence fluctuating vertical velocity. The two mechanisms of turbulence play important roles in two different particle size domains. As shown by Guha [1997] and Young and Leeming [1997], while the turbulent diffusion, together with the Brownian diffusion, is most efficient for small particles in the range of diffusion domain, the burst effect of turbulence dominates the diffusion-impaction and inertial-moderated regimes.

[9] The burst effect of turbulence on dry deposition of particles can be described by a partial differential equation [Guha, 1997; Young and Leeming, 1997]. The equation can be solved for some types of pipe flows, however, it is almost impossible to apply it directly to atmospheric surface flows, given the complexities of the atmospheric boundary turbulence and the irregularity of the Earth's surface. In the following, we refer to dry deposition velocity due to the burst effect of turbulence as turbo velocity. A simplified form of it for a flow over a ground surface is [Caporaloni *et al.*, 1975; Guha, 1997; Young and Leeming, 1997]

$$V_{tb} = -\tau_p \frac{d\overline{v_{pz}^2}}{dz}, \quad (3)$$

where  $\tau_p$ ,  $\overline{v_{pz}^2}$  are the relaxation time and the vertical component of the velocity fluctuation of a particle.  $\overline{v_{pz}^2}$  can

be related to  $v_z'$ , the  $z$  component of the fluctuation of the surface flow, as [Guha, 1997]

$$\overline{v_{pz}^2} = v_z'^2 / (1 + 0.7(\tau_p/T_L)), \quad (4)$$

where  $T_L$  is the Lagrangian timescale of a surface flow.

[10] Therefore, the turbo velocity can be expressed as

$$V_{tb} = -\tau_p \left( \frac{T_L}{T_L + 0.7\tau_p} \right)^2 \frac{d\overline{v_z'^2}}{dz}. \quad (5)$$

Even expressed in this analytical form, an explicit calculation of the turbo velocity is not easy for an atmospheric surface flow. However, from this expression we can gain some insights on how this velocity is affected physically by some characteristic variables. For this purpose, we use the conceptual model of the atmospheric boundary flow and assume that the atmospheric surface flow is made up of two layers: an aerodynamic layer and a viscous sublayer just adjacent to the ground surface. In the aerodynamic layer we assume that  $\overline{v_z'^2}$  does not vary with height [Rodean, 1996]. In the viscous sublayer  $\overline{v_z'^2}$  decreases monotonically until it reaches zero at the surface. Approximations can then be made of

$$\begin{aligned} V_{tb} &= -\tau_p \left( \frac{T_L}{T_L + 0.7\tau_p} \right)^2 \frac{d\overline{v_z'^2}}{dz} \\ &= -\tau_p \left( \frac{T_L}{T_L + 0.7\tau_p} \right)^2 \frac{\sigma_w^2 - 0}{\delta z} = -\tau_p \left( \frac{T_L}{T_L + 0.7\tau_p} \right)^2 \frac{\sigma_w^2}{\delta z}, \end{aligned} \quad (6)$$

where  $\delta z$  is the depth of the viscous sublayer; and  $\sigma_w^2$  is the  $z$  component of the flow velocity variance and can be approximated as  $2u_*^2$  [Rodean, 1996]. Dependence of  $V_{tb}$  on  $\tau_p$ , and therefore on particle size, can be neglected when  $\tau_p \gg T_L$ . The depth of the viscous sublayer is affected by surface roughness and friction velocity. An increase of either of them tends to make the sublayer thinner [Lai *et al.*, 2001; Young and Leeming, 1997]. Therefore, surface roughness length  $z_0$  and friction velocity  $u_*$  could be the two most characteristic variables for describing turbo velocity. In the next subsection, a parameterization of turbo velocity using these two variables will be presented.

## 2.3. Development of a New Size-Resolved Dry Deposition Model

[11] On the basis of observed dry deposition velocities for particles in vertical pipes, Muyschondt *et al.* [1996] developed an empirical model, which includes a dry deposition velocity term due to the effect of turbulence. Following the work of Muyschondt *et al.* [1996], Noll *et al.* [2001] proposed a size-resolved model for dry deposition in the atmosphere.

[12] The dimensionless dry deposition velocity of particles on vertical pipe walls is parameterized as [Muyschondt *et al.*, 1996]

$$V_d/u_* = a_1 e^{-0.5[(Re-a_2)/a_3]^2} + a_4 e^{-0.5[(\ln \tau^+ - \ln a_5)/a_6]^2}, \quad (7)$$

where  $Re$  is the flow Reynolds number, and  $\tau^+$  is the dimensionless relaxation time.  $Re$  is defined as  $UL/\nu$ , where



$U$  is the mean flow velocity in a pipe,  $L$  is the characteristic scale length of a pipe, and  $\nu$  is the air kinematic viscosity.  $\tau^+$  is defined as  $\tau^+ = \frac{\tau u_*^2}{\nu}$ , where  $\tau$  is the particle relaxation time. The regression coefficients are  $a_1 = 0.0226$ ,  $a_2 = 40300$ ,  $a_3 = 15330$ ,  $a_4 = 0.1394$ ,  $a_5 = 49.0$ ,  $a_6 = 1.136$ .

[13] The same form is used by *Noll et al.* [2001] to parameterize the dimensionless dry deposition velocity of atmospheric aerosols onto the ground surface, on the basis of observations conducted in different meteorological conditions, but with different regression coefficients. The dimensionless dry deposition velocity is expressed as

$$V_d/u_* = b_1 e^{-0.5[(Re-b_2)/b_3]^2} + b_4 e^{-0.5[(\ln \tau^+ - \ln b_5)/b_6]^2}, \quad (8)$$

where  $b_1 = 0.02418$ ,  $b_2 = 40,300.0$ ,  $b_3 = 3,833.25$ ,  $b_4 = 1.49115$ ,  $b_5 = 18.0$ ,  $b_6 = 1.7$ .

[14] It is worth noting that  $b_2$  equals  $a_2$ , and  $b_1$  is almost equal to  $a_1$ . These equalities indicate some similarities between the deposition of particles in pipes and that in the atmosphere. The dry deposition velocity in these two models is made up of two terms. The first term is a function of the Reynolds number only and describes the turbulence effect, while the second term is a function of the dimensionless relaxation time only and describes the inertial impaction effect.

[15] *Muyshondt et al.* [1996] originally developed their model mainly as an empirical one. They attributed the Reynolds term to the turbulence diffusion. However, the component of the dry deposition velocity due to the Brownian and turbulence diffusion decreases with the dimensionless relaxation time near exponentially and makes little contribution to the total dry deposition velocity for the dimensionless relaxation time in the range of 0.1 to 10 [Guha, 1997], while from the observation data, the contribution to the dry deposition due to turbulence is very significant for this particle size range when the Reynolds number is large [Muyshondt et al., 1996; Noll et al., 2001]. The Reynolds number defined by *Muyshondt et al.* [1996] uses the mean pipe flow velocity. This mean velocity is directly related to the friction velocity of the pipe flow, and can be further related to the radial velocity fluctuation of the pipe flow,  $v'_r$ , as  $v'_r/u_*$  is nearly a constant in the core region of the pipe flow. Since  $v'_r$  is a major characteristic variable in describing the burst effect of turbulence (see the equation in section 2.2), we believe that the Reynolds term in *Muyshondt et al.*'s model includes the contribution from both the burst effect and diffusion of turbulence, and that the former one makes the major contribution for a large Reynolds number.

[16] In the model of *Noll et al.* [2001], the Reynolds number is defined as  $UL/\nu$ , where  $U$  is the wind velocity above the deposition disk used to collect the deposited particles,  $L$  is the characteristic length of the disk, and  $\nu$  is the kinematic viscosity of the air. Since characteristics of the atmospheric wind turbulence are determined by variables more characteristic of the wind fields and the underline surfaces, we introduce a roughness Reynolds number  $Re^*$  to describe the atmospheric turbulence above the ground surface. This is also supported by the conclusion of *Webb* [1979] that one must use the roughness Reynolds number

instead of the Reynolds number as the characteristic flow variable to better understand the turbulent effects of rough surfaces.  $Re^*$  is defined as  $u_* z_0/\nu$ , where  $u_*$  is the friction velocity, a characteristic variable of the surface wind field; and  $z_0$  is the roughness length of the surface, a characteristic variable to describe the turbulent effect due to the surface roughness. The roughness Reynolds number determines the roughness of the wind flow above the ground surface; the higher the number, the more turbulent the flow. The experimentally determined criteria for smooth or rough flow is [Brutsaert, 1982; Seinfeld and Pandis, 2006]

$$Re^* \begin{cases} < 0.13 & \text{smooth flow} \\ > 2.5 & \text{rough flow} \end{cases}$$

[17] To build a new dry deposition model, we replace the Reynolds number term in the model of *Noll et al.* [2001] with a new term which is a function of the roughness Reynolds number. In the model of *Noll et al.*, the coefficients for the Reynolds term were derived from regression with  $Re$ . The ratio of  $Re^*$  to  $Re$  is  $u_* z_0/UL$ . In their study,  $u_*/U$  was set to be 0.028, and  $L$  was taken to be 0.05 m. The site of their field experiment was located in a mixed institutional, commercial, and residential area. The typical  $z_0$  for such an area is about 2 m. So for *Noll et al.*,  $Re^*$  is linearly correlated with  $Re$ .

[18] There are 3 coefficients for the Reynolds term in the models of *Muyshondt et al.* [1996] and *Noll et al.* [2001]. The first one ( $a_1$  or  $b_1$ ) is the maximum contribution to the dimensionless dry deposition velocity that the Reynolds term can make. The derived coefficient from the two models is very close (0.023 versus. 0.024). The second coefficient ( $a_2$  or  $b_2$ ) is the "saturated Reynolds number." When increasing the Reynolds number to this value, the Reynolds term reaches its maximum. Both models set this coefficient at 43000. The third coefficient ( $a_3$  or  $b_3$ ) determines how steeply the Reynolds term increases with the Reynolds number. The main difference in the derived coefficients for the two models is the third coefficient. In this study, both  $a_3$  and  $b_3$  are tested with observations data (section 5) and it is found that  $a_3$  fits the data better. Therefore, we adopt the regression coefficients from the model of *Muyshondt et al.* [1996] for this Reynolds term. We take from the model of *Noll et al.* the term of dimensionless relaxation time, which describes the contribution of inertial impaction to dry deposition. After reviewing the observation data conducted at the same site from *Aluko and Noll* [2006], the regression coefficient  $b_4$  is replaced with  $0.6b_4$  to take into account of the underestimation of  $u_*$  by *Noll et al.* [2001]. For the contribution of Brownian diffusion to dry deposition, which is more significant for aerosol particles with diameters of less than  $0.1 \mu\text{m}$ , we adopt the parameterization from *Slinn and Slinn* [1980] and expressed as  $u_* Sc^{-0.6}$ , where  $Sc$  is the dimensionless Schmidt number ( $Sc = \nu/D$ , and  $D$  is the particle diffusion coefficient). The new general formula of the surface dry deposition velocity is

$$V_{ds} = u_* \left\{ Sc^{-0.6} + c_1 e^{-0.5[(Re^*-c_2)/c_3]^2} + c_4 e^{-0.5[(\ln \tau^+ - \ln c_5)/c_6]^2} \right\}, \quad (9)$$

where  $c_1 = 0.0226$ ,  $c_2 = 40,300$ ,  $c_3 = 15,330$ ,  $c_4 = 0.8947$ ,  $c_5 = 18$ ,  $c_6 = 1.7$ . When  $Re^*$  is greater than  $c_2$ , it is set to be equal to  $c_2$ .

[19] In summary, the new model of dry deposition velocity is made up of three terms. The first term is due to the Brownian diffusion, and is a function of the Schmidt number; the second term is a contribution from the burst effect of eddy turbulence, and is a function of the roughness Reynolds number; and the third term is due to the inertial impaction, and is a function of the dimensionless relaxation time.

[20] Another commonly used dimensionless number to describe the inertial impaction is the Stokes number, which is defined as  $St = \frac{V_t u_*^2}{g\nu}$  [Zhang *et al.*, 2001; Giorgi, 1986].

Recall that for aerosol particles with diameters of less than a few tens of micrometers ( $\sim 30 \mu\text{m}$ ),  $V_t = \tau g$ ; therefore, we have  $St = \tau u_*^2 / \nu$ . So the Stokes number is the same as the dimensionless relaxation time for particles with diameters of less than  $30 \mu\text{m}$ . We name the first term in the new model the Brownian term, or the Schmidt term; the second term the turbulence term, or the Reynolds term; and the third term the inertial term, or the Stokes term.

[21] In the following analysis, we neglect the aerodynamic resistance (a case of neutral boundary condition and  $V_d$  is defined at the height of  $z_0$ ), and we have  $V_d = V_t + V_{ds}$ . The particle density is assumed to be  $10^3 \text{ kg m}^{-3}$  in calculating dry deposition velocities in the following sections.

### 3. Sensitivity Analysis of the New Dry Deposition Model

#### 3.1. Sensitivity to Friction Velocity

[22] Figures 1a–1e show size-resolved dry deposition velocities calculated with the new model under different friction velocities for roughness lengths ranging from 0.01 m to 5 m. According to McRae *et al.* [1982], the surface of a lawn typically has a roughness length of 0.01 m, and the surface of a typical central business district has a roughness length of 5 to 10 m. For the same roughness length, the dry deposition velocity increases with the friction velocity for the whole size range. This is because the three terms of the dry deposition velocity all increase with the increase of the friction velocity. The friction velocity affects the Brownian term linearly because the dimensionless Brownian term does not depend on the friction velocity. The dimensionless Reynolds term increases with the Roughness Reynolds number, which is in proportion to the friction velocity. The dimensionless Stokes term increases with the Stokes number, which is in proportion to the square of the friction velocity.

#### 3.2. Sensitivity to Surface Roughness Length

[23] The sensitivity of dry deposition velocity to surface roughness length is shown in Figures 2a–2d. Roughness length affects the dry deposition velocity only through the Reynolds term, and mainly in the size range from  $0.01 \mu\text{m}$  to a few micrometers. The dimensionless Reynolds term is a function of the roughness Reynolds number, which is in proportion to the product of the friction velocity and the roughness length. Therefore, the sensitivity of the dry deposition velocity to the roughness length depends on the value of friction velocity. For example, for a friction velocity of  $0.1 \text{ m s}^{-1}$  (Figure 2a), the dry deposition

velocity is not sensitive to the variation of roughness length from 0.01 m to 1 m, but significantly increases with the roughness length when the roughness length increases from 1 m to 5 m. For a friction velocity of  $1 \text{ m s}^{-1}$  (Figure 2d), there is a negligible difference in the dry deposition velocity when the roughness length changes from 1 m to 5 m, but when the roughness length changes from 0.1 m to 1 m, the increase of the dry deposition velocity is around one order of magnitude. Figure 3 shows that the dimensionless Reynolds term increases rapidly with the roughness Reynolds number when it increases from 1000 to 42000. Only when the roughness Reynolds number falls into this range, the Reynolds term is sensitive to the roughness length.

#### 3.3. Sensitivity to Particle Size

[24] The sensitivity of dry deposition velocity to particle size is very obvious as shown in Figures 1 and 2. Figures 4a and 4b show the contribution to the dry deposition velocity from each deposition mechanism for two typical surface roughness lengths and wind friction velocities. In Figure 4a, a roughness length of 5 cm is typical of a surface with uncut grass, and a friction velocity of  $0.2 \text{ m s}^{-1}$  usually corresponds to a light surface wind. In Figure 4b a roughness of 0.5 m is typical of a surface covered with low trees and a friction velocity of  $0.5 \text{ m s}^{-1}$  usually corresponds to a medium surface wind. Also shown in Figures 4a and 4b are the upper and lower limits of the roughness Reynolds term, which describes the maximum and minimum contributions that the eddy turbulence effect can make. Depending on the value of the roughness length, the eddy turbulence effect is a major contribution to the total dry deposition velocity for particles with sizes in the range of  $0.01 \mu\text{m}$  up to a few micrometers. Above around a few micrometers, the dry deposition velocity is dominated by the inertial impaction term, and in this range the Brownian and the eddy turbulence terms can be neglected. The inertial impaction term has also been parameterized by Slinn and Slinn [1980], using the Stokes number, as  $u_* 10^{-3/St}$ , and this parameterization was recently reconfirmed by the observations conducted by Aluko and Noll [2006] for large airborne particles (diameter greater than  $8 \mu\text{m}$ ). As shown in Figure 5, the Stokes term of the current model agrees very well with Slinn and Slinn's model for particle sizes of greater than  $8 \mu\text{m}$ , while for particles with diameters of less than about  $8 \mu\text{m}$ , the dry deposition velocity of Slinn and Slinn's model is significantly lower than the one in the current model.

[25] Figures 4a and 4b show that for particles with sizes between 1 and  $8 \mu\text{m}$ , the dry deposition is controlled by the Reynolds and Stokes terms. This was also pointed out by Noll *et al.* [2001]. When the particle size decreases to the submicron range, the Stokes term drops quickly and is dominated by the Reynolds term. When the particle size decreases further, the Brownian term picks up and dominates the Reynolds term. In the size range from  $0.01 \mu\text{m}$  to  $1 \mu\text{m}$ , the dry deposition velocity is mainly controlled by the roughness Reynolds number and the Schmidt number, with the relative importance depending on the roughness Reynolds number. For particles with diameters of less than 10 nanometers, the dry deposition is determined by the Schmidt number only.

[26] In summary, the dry deposition velocity depends on the particle size, the friction velocity of the wind turbulence

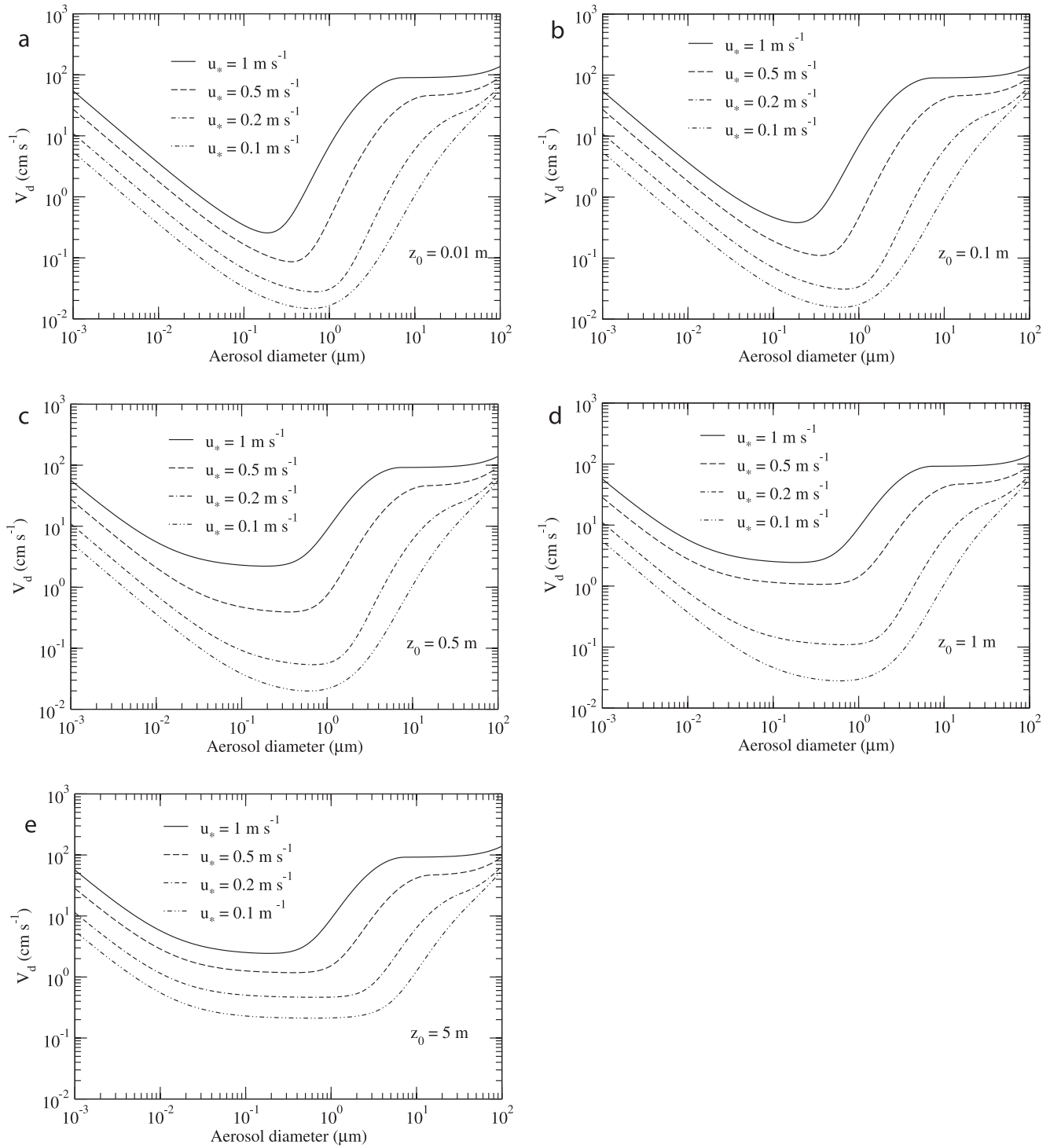


**Figure 1.** Size-resolved dry deposition velocities of different friction velocities for surface roughness lengths ranging from 0.01 to 5 m.

and the roughness length of the surface. For the same particle size, the higher the friction velocity and the rougher the ground surface, the larger the dry deposition velocity is. For the same wind turbulence and ground surface, the dry deposition decreases with the increase of particle size in the aerosol nuclei mode ( $10^{-3} \sim 0.1 \mu\text{m}$ ), reaches a minimum in the aerosol accumulation mode ( $0.1 \sim 2.5 \mu\text{m}$ ), and then

increases with the particle size until the particles are settled at the terminal velocities.

#### 4. Four-Mode Parameterization

[27] The dry deposition velocity is significantly size-dependent. The mass-averaged mean dry deposition velocity in each aerosol mode is quite different. The trend of the

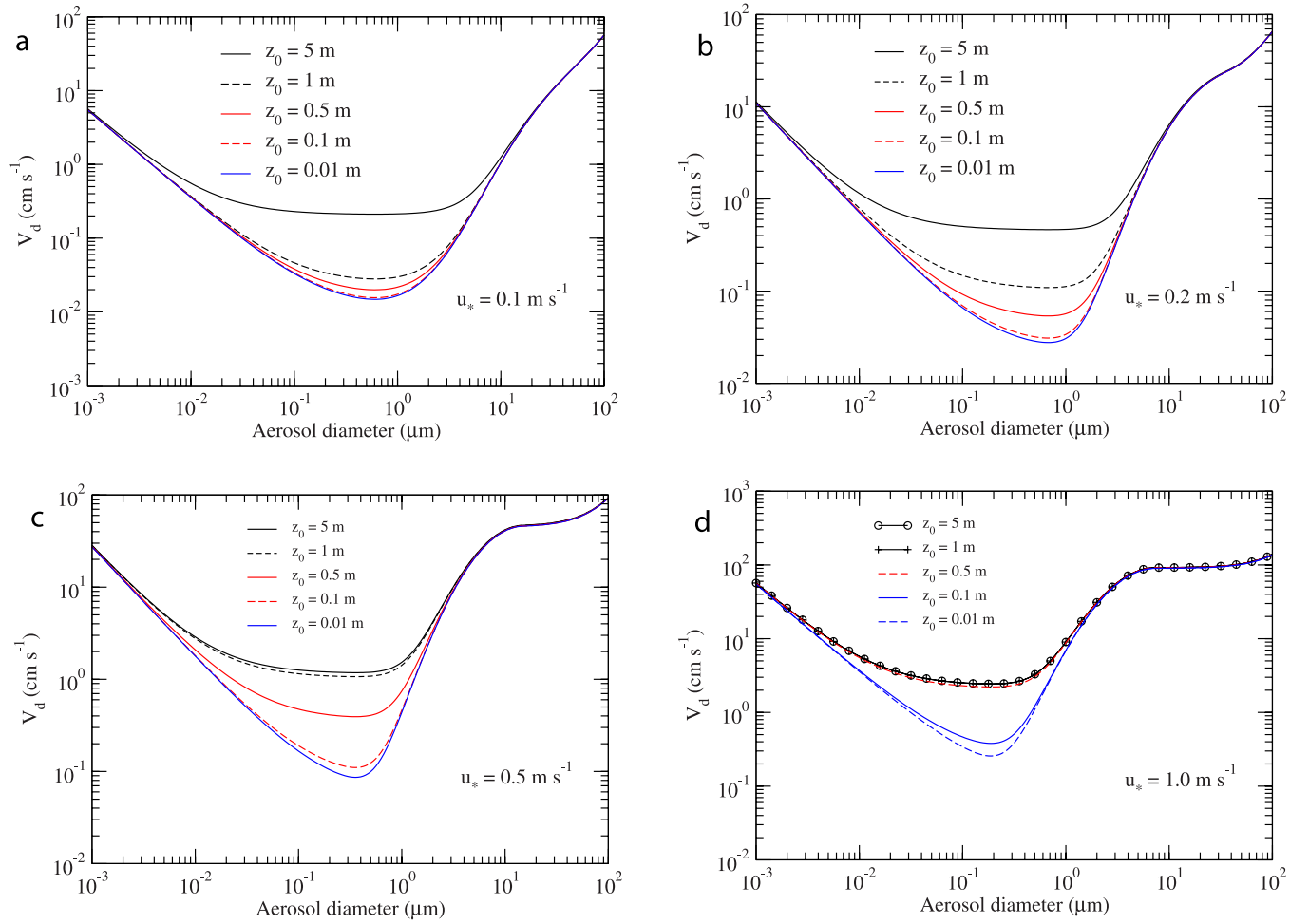


**Figure 2.** Size-resolved dry deposition velocities of different roughness lengths for friction velocities ranging from 0.1 to 1.0 m s<sup>-1</sup>.

dry deposition velocity with particle size shows a similarity to the below-cloud scavenging coefficients [Feng, 2007]. Applying the same idea of the three-mode parameterization of below-cloud scavenging [Feng, 2007], we propose a four-mode parameterization of dry deposition for use in atmospheric transportation and dispersion models. The four modes of the aerosol size spectrum are defined as

$$\begin{cases} \text{Nuclei mode } 0.001 < dp \leq 0.1 \text{ } \mu\text{m} \\ \text{Accumu. mode } 0.1 < dp \leq 2.5 \text{ } \mu\text{m} \\ \text{Coarse mode } 2.5 < dp \leq 10 \text{ } \mu\text{m} \\ \text{Giant mode } 10 < dp \leq 100 \text{ } \mu\text{m} \end{cases}$$

For each mode, the mass-averaged surface dry deposition velocity is

$$V_{dsi} = \frac{\int_{d_{li}}^{d_{2i}} d_p^3 V_{ds}(d_p) n(d_p) dd_p}{\int_{d_{li}}^{d_{2i}} d_p^3 n(d_p) dd_p}, \quad (10)$$

where  $d_p$  is the particle diameter and  $n(d_p)$  is the particle number size distribution. In this study, we use the aerosol size distribution model suggested by Jaenicke [1993]. For

each aerosol type, the Jaenicke model of size distribution is a sum of 3 lognormal distributions, as follows

$$n_N(\log D_p) = \sum_{i=1}^3 \frac{N_i}{(2\pi)^{1/2} \log \sigma_i} \exp\left(-\frac{(\log D_p - \log \bar{D}_{pi})^2}{2 \log^2 \sigma_i}\right), \quad (11)$$

where  $N$ ,  $\bar{D}_p$ , and  $\sigma$  are specific coefficients for each type of aerosol.

[28] Since the Reynolds term of the surface dry deposition velocity is not a function of the particle size, we can separate the surface dry deposition velocity into two terms as follows:

$$V_{ds} = V_{d1} + V_{d2}, \quad (12)$$

where

$$V_{d1} = u_* c_1 e^{-0.5[(Re^* - c_2)/c_3]^2} \quad (13)$$

and

$$V_{d2} = u_* \left\{ Sc^{-0.6} + c_4 e^{-0.5[(\ln \tau^+ - \ln c_5)/c_6]^2} \right\}. \quad (14)$$

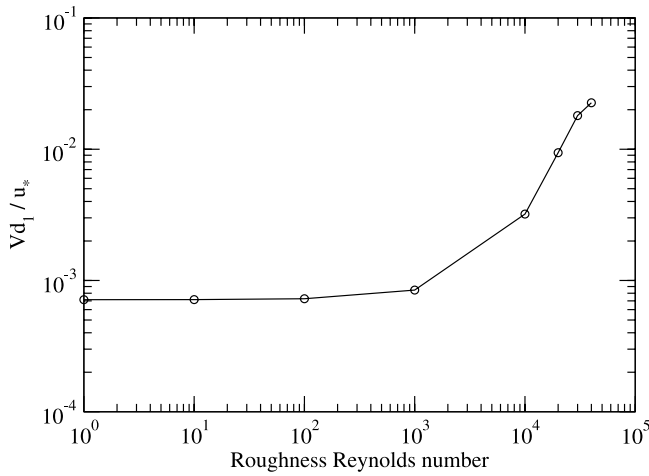


**Figure 3.** Relationship between the dimensionless Reynolds term and the roughness Reynolds number.

[29] After integrating over the particle diameter, the surface dry deposition velocity in each mode can be expressed as  $V_{dsi} = V_{d1} + V_{d2i}(u_*)$ , where  $V_{d2i}(u_*)$  is a regression function. As an example, Figure 6 shows corre-

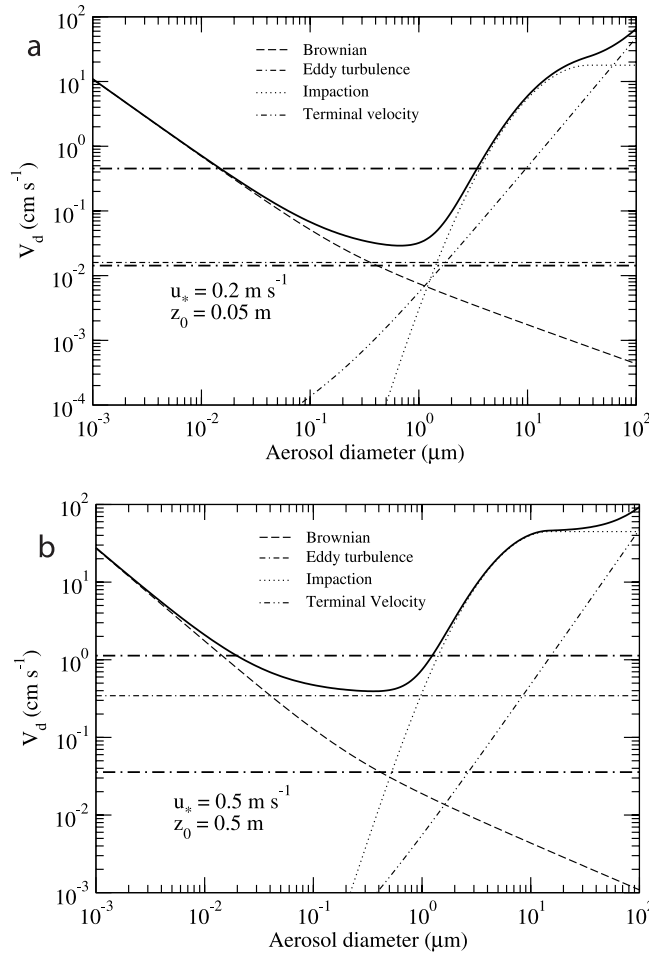


**Figure 4.** Size-resolved dry deposition velocities for different friction velocity and surface roughness length. The bold dot-dashed lines are the upper and lower limits of the roughness Reynolds term.

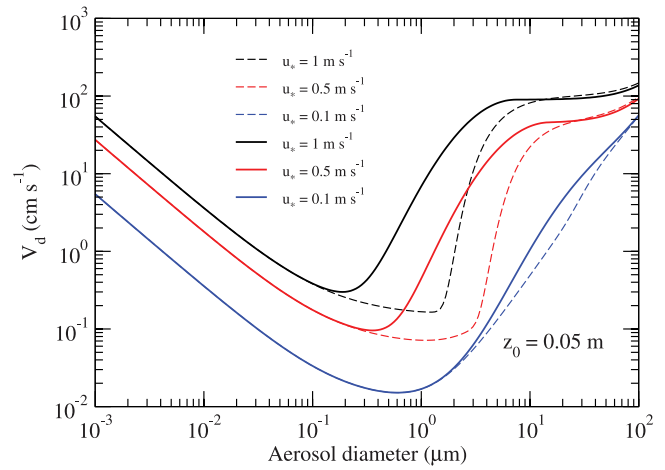


**Figure 5.** Size-resolved dry deposition velocity for  $z_0 = 0.05$  m. Solid lines are for the current model; dashed lines are for the current model with the Stokes term being replaced with Slinn and Slinn's parameterization  $u_* 10^{-3/st}$ .

lations between  $V_{d2}$  and  $u_*$  for remote continental aerosol. For each mode, there is a very good power law relationship between  $V_{d2}$  and  $u_*$  with  $R^2 \geq 0.96$ . We parameterize  $V_{d2i} = a_i u_*^{b_i}$ , where  $a_i$  and  $b_i$  are regression coefficients, and are listed in Table 1 for each aerosol mode and aerosol type.

[30] For each aerosol mode, correlations between  $V_{d2}$  and  $u_*$  for each aerosol type are shown in Figures 7a–7d. For the nuclei mode, the urban aerosol has the largest dry deposition velocity and the polar aerosol has the smallest one.  $V_{d2}$  increases with  $u_*$  linearly. For a typical friction velocity of  $0.4 \text{ m s}^{-1}$ ,  $V_{d2}$  is between  $0.12$  and  $0.22 \text{ cm s}^{-1}$ . For the accumulation mode, we only show the correlations for 3 types of aerosol to make the graph easier to read. For the same friction velocity, the dry deposition velocity for the urban aerosol is the smallest and the one for the desert aerosol is the largest. For a friction velocity of  $0.4 \text{ m s}^{-1}$ , the dry deposition velocity is between  $0.2 \text{ cm s}^{-1}$  and  $1 \text{ cm s}^{-1}$ . The dry deposition velocity is not very sensitive to the aerosol type in the coarse mode. For a friction velocity of

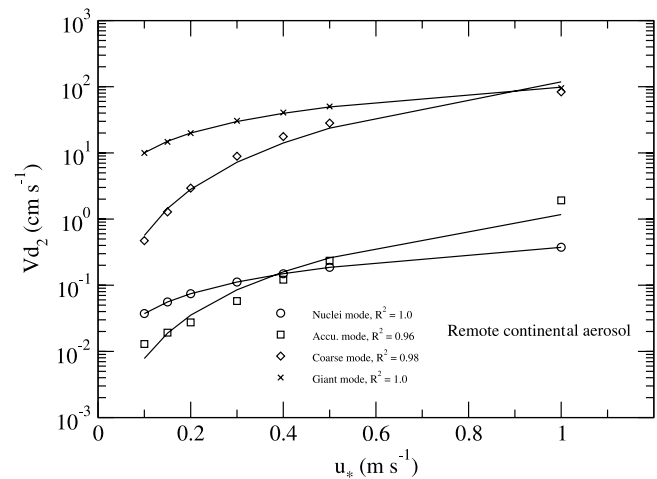


**Figure 6.** Bulk dry deposition velocity versus friction velocity in each aerosol mode for remote continental aerosol.



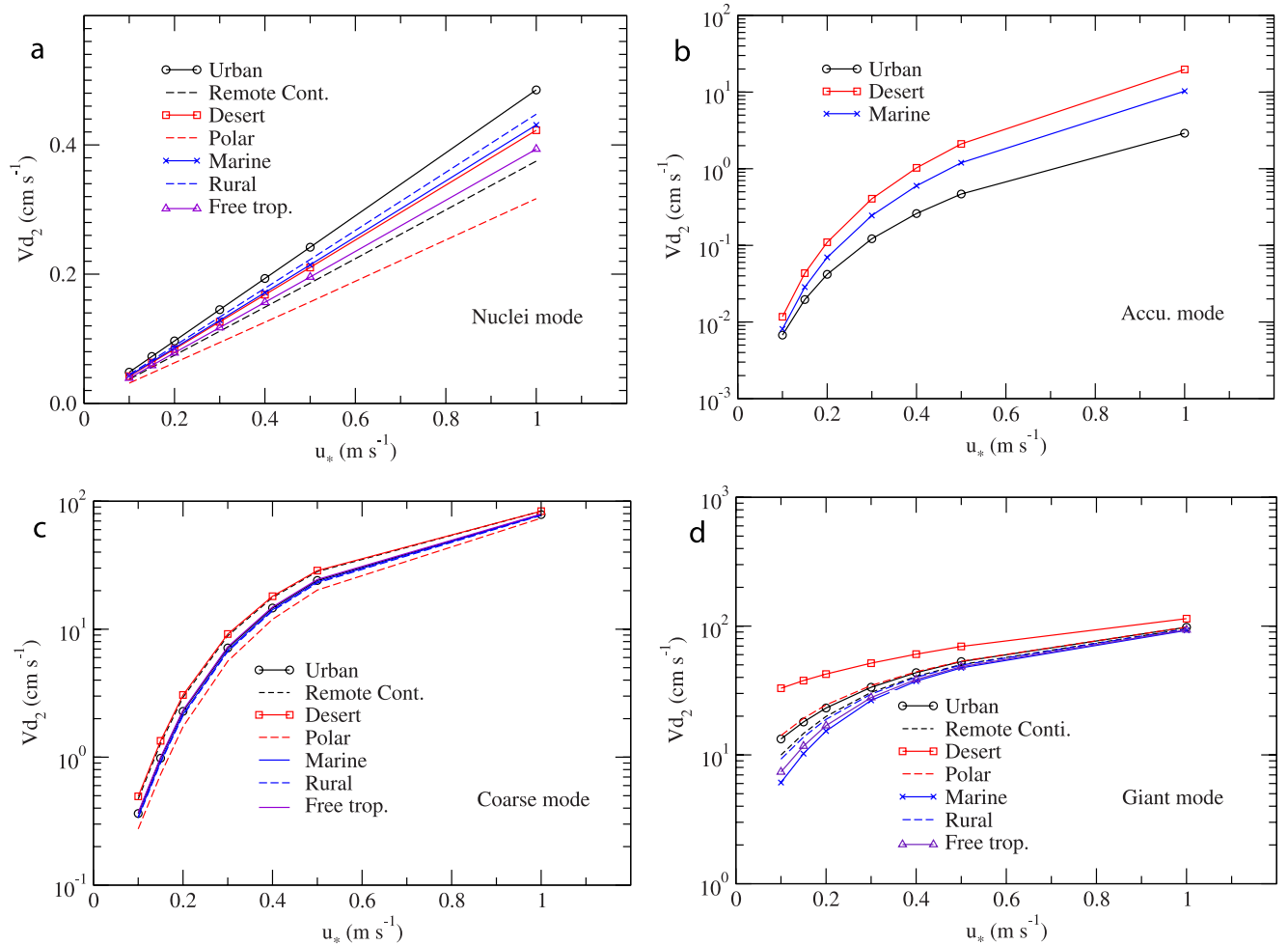
**Table 1.** Coefficients of Power Law Regression  $V_{d2} = au_*^b$  for the Whole Aerosol Size Spectrum and for Four Modes

	Bulk Parameteriza- tion for the Whole Size Range		Mode 1		Mode 2		Mode 3		Mode 4	
	$a$	$b$	$a$	$b$	$a$	$b$	$a$	$b$	$a$	$b$
Urban	0.5256	1.4449	0.0048	1.0000	0.0315	2.7925	1.2891	2.6878	1.0338	1.2644
Remote Conti.	0.8191	1.4467	0.0037	1.0000	0.0120	2.2413	1.3977	2.5838	1.0707	1.3247
Desert	0.9138	1.0405	0.0042	1.0000	0.2928	3.8581	1.3970	2.5580	0.9155	1.0364
Polar	0.7537	1.3234	0.0032	1.0000	0.1201	3.4407	1.1838	2.8033	1.0096	1.2069
Marine	0.8132	1.8476	0.0043	1.0000	0.1337	3.5456	1.2834	2.7157	1.1595	1.4863
Rural	0.6886	1.6545	0.0045	1.0000	0.0925	3.2920	1.2654	2.7227	1.0891	1.3654
Free Trop.	0.9454	1.6994	0.0039	1.0000	0.2859	3.8558	1.3072	2.6840	1.1242	1.4240

$0.4 \text{ m s}^{-1}$ , the dry deposition velocity is between about 10 and  $20 \text{ cm s}^{-1}$ . However, in this mode, the dry deposition velocity increases considerably with the friction velocity. As the friction velocity increases from  $0.2 \text{ cm s}^{-1}$  to  $0.4 \text{ cm s}^{-1}$ , the dry deposition velocity increases by about an order of magnitude. Desert aerosol shows a much higher dry deposition velocity in the giant mode (Figure 7d) than all the other types of aerosol because desert aerosol has a higher percentage of mass in larger particle sizes.

[31] The above four-mode dry deposition parameterization can be implemented into atmospheric dispersion models following the method of Feng [2007]. For each aerosol mode, the bulk dry deposition velocity can be defined as

$$\bar{V}_{di} = \bar{V}_{ti} + \frac{1}{R_a + 1/\left(V_{d1} + a_i u_*^{b_i}\right)}, \quad (15)$$

**Figure 7.** Correlations between dry deposition velocity ( $V_{d2}$ ) and friction velocity in each aerosol mode for different types of aerosol.

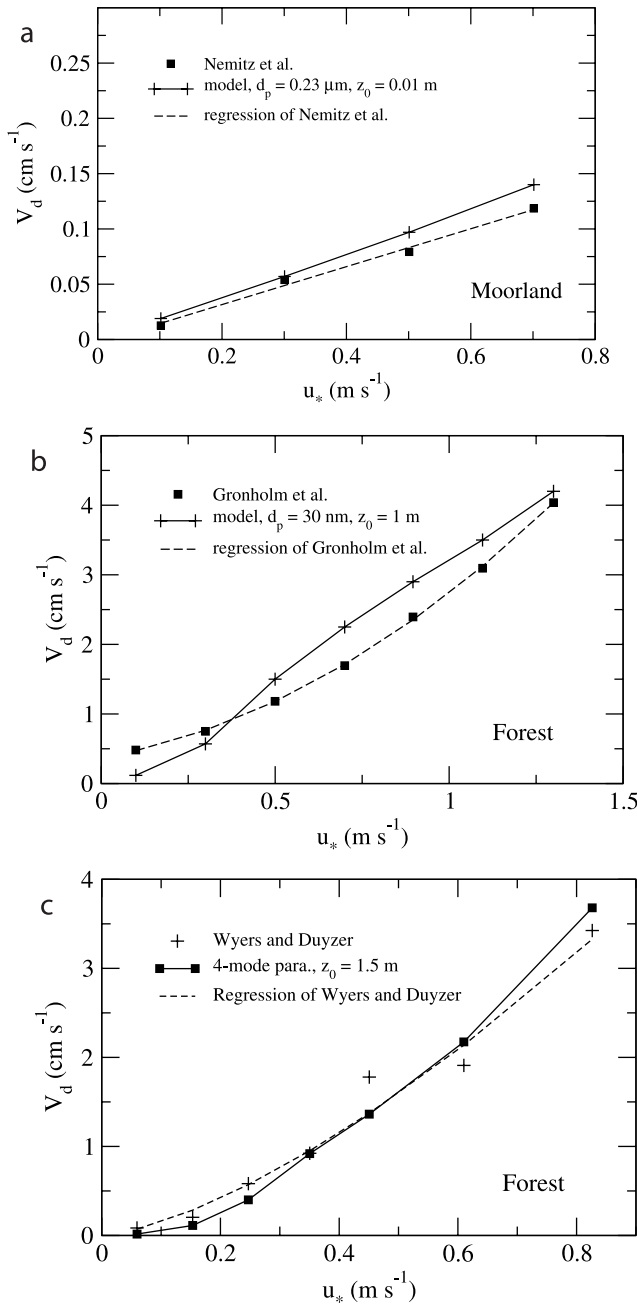


**Figure 8.** Comparisons of measured dry deposition velocities with predictions of the new dry deposition model and the four-mode parameterization: (a) *Nemitz et al.* [2002], (b) *Grönholm et al.* [2007], and (c) *Wyers and Duyzer* [1997].

where  $\bar{V}_{ti}$  is the bulk terminal velocity for each aerosol mode, and

$$\bar{V}_{ti} = \frac{\int_{d_{li}}^{d_{hi}} d_p^3 V_t(d_p) n(d_p) dd_p}{\int_{d_{li}}^{d_{hi}} d_p^3 n(d_p) dd_p}; \quad (16)$$

$R_a$  is the aerodynamic resistance and is defined in section 2; and

$$V_{d1} = u_* c_1 e^{-0.5[(Re-c_2)/c_3]^2}. \quad (17)$$

## 5. Comparisons With Measured Dry Deposition Velocities

[32] Over the past three decades, there have been many field measurements of dry deposition of particles over different surfaces. In this section, some of these measurements are used to compare with predictions of dry deposition velocity from the newly developed dry deposition model and the four-mode parameterization. When values of friction velocity and roughness length are not available from the original reports, typical values for them are assumed. For most cases, to compare with measured mean dry deposition velocities, we assume the typical mean friction velocity to be 0.2–0.3 m s<sup>−1</sup>; to compare with measured ranges of dry deposition velocity, we assume the typical range of friction velocity to be 0.2–0.6 m s<sup>−1</sup>. For the grass, moorland, forest, urban, and snow surfaces, the typical roughness length is taken to be 0.05, 0.01, 1.5, 5, and 10<sup>−3</sup> m respectively [*McRae et al.*, 1982], unless it is otherwise specified. The number size distribution of urban aerosol is assumed in applying the four-mode parameterization. The comparisons between the measured dry deposition velocities reported in the literature and the ones predicted by the model are presented in Figure 8 and Table 2.

[33] For a grass surface, measurements of dry deposition velocities have been conducted in several field studies. As shown in Table 2, in general, the predictions by the new dry deposition model are in good agreement with the measurements. For example, For sulphate aerosols, *Allen et al.* [1991] observed a mean  $V_d$  of 0.1 cm s<sup>−1</sup>; *Doran and Droppo* [1983] observed mean  $V_d$  of 0.2–0.3 cm s<sup>−1</sup> and some cases of 0.3–0.4 cm s<sup>−1</sup>; *Hicks et al.* [1983] observed a diurnal average of 0.2 cm s<sup>−1</sup> and a daytime average of 0.7 cm s<sup>−1</sup>. Sulphate aerosols are mainly in the accumulation mode. If we assume the size distribution of sulphate aerosols follows that of urban aerosols, on the basis of the four-mode parameterization (mode 2), we have  $V_d = 0.05, 0.14, 0.28$  and  $0.82$  cm s<sup>−1</sup> for  $u_* = 0.2, 0.3, 0.4$ , and  $0.6$  m s<sup>−1</sup> respectively. The measured range of  $V_d$  agrees well with the one predicted by the model. In *Hicks et al.*'s [1983] measurements, a higher daytime mean  $V_d$  corresponds to a higher daytime  $u_*$ .

[34] For a moorland surface, Figure 8a presents a comparison of dry deposition velocity between the model prediction and the measured one from *Nemitz et al.* [2002] for aerosol particles with diameters of 0.22–0.24 μm. The observed variation of dry deposition velocity with friction velocity is well captured by the model.

[35] For a forest surface, Figures 8b and 8c present comparisons between model predictions and measured dry deposition velocities from *Grönholm et al.* [2007] and *Wyers and Duyzer* [1997], respectively. *Grönholm et al.* [2007] measured dry deposition velocities of aerosol particles with  $d = 30$  nm over a pine forest. Figure 8b shows that the model overestimates the measurements a little bit when  $u_* > 0.3$  m s<sup>−1</sup>. Part of the reason for this overestimation is due to the aerosol emission, which makes the

**Table 2.** Comparisons of Dry Deposition Velocity Between Measurements and Predictions of the Model and the Parameterization

Reference	Measurement		Model	
	Size or Size Range, $\mu\text{m}$	$V_{ds}$ cm s <sup>-1</sup>	$V_{ds}$ cm s <sup>-1</sup>	Model Parameters
<i>Grass, <math>z_0 = 0.05</math> m</i>				
Garland [1981]	0.04	0.30	0.23	$u_* = 0.3$ m s <sup>-1</sup> $D_p = 0.04$ $\mu\text{m}$
Gallagher et al. [2002] Dorsey [2002]	0.1–0.2	0.087–0.113	0.08–0.13	$u_* = 0.3$ – $0.5$ m s <sup>-1</sup> $D_p = 0.15$ $\mu\text{m}$
Vong et al. [2004]	0.34	0.22	0.10	$u_* = 0.5$ m s <sup>-1</sup>
	0.52	0.18	0.11	$u_* = 0.5$ m s <sup>-1</sup>
	0.84	0.22	0.28	$u_* = 0.5$ m s <sup>-1</sup>
Garland [1981]	1.8	0.05–0.12	0.04–0.10	$u_* = 0.15$ – $0.4$ m s <sup>-1</sup> $D_p = 1.8$ $\mu\text{m}$
Allen et al. [1991]	Accumulation mode (sulphate)	0.1	0.05–0.82	$u_* = 0.2$ – $0.6$ m s <sup>-1</sup>
Doran and Droppo [1983]		0.2–0.3	0.05	$u_* = 0.2$ m s <sup>-1</sup>
			0.14	$u_* = 0.3$ m s <sup>-1</sup>
			0.28	$u_* = 0.4$ m s <sup>-1</sup>
			0.82	$u_* = 0.6$ m s <sup>-1</sup>
Hicks et al. [1983]		0.2 (diurnal mean) 0.7 (daytime mean)		four-mode para., mode 2
<i>Forest, <math>z_0 = 1.5</math> m</i>				
Hicks et al. [1982]	0.03–0.1	0.5–2.0	0.28–1.6	$u_* = 0.2$ – $0.6$ m s <sup>-1</sup> four-mode para., mode 1
Hicks et al. [1989]	0.05–0.1	0.8	0.69	$u_* = 0.3$ m s <sup>-1</sup> four-mode para., mode 1
Lamaux et al. [1994]	0.05–1.0	0.05–0.6	0.07–1.5	$u_* = 0.15$ – $0.5$ m s <sup>-1</sup> four-mode para., mode 2
Gallagher et al. [2002]	0.1–0.2	0.21	0.22	$u_* = 0.25$ m s <sup>-1</sup> $D_p = 0.15$ $\mu\text{m}$ $z_0 = 1.0$ m
Gallagher et al. [1997]	0.1–3.0	0.01–10.0	0.1–2.1 5.4	$u_* = 0.15$ – $0.6$ m s <sup>-1</sup> $u_* = 1.0$ m s <sup>-1</sup> four-mode para., mode 2
Horvath [2003]	PM2.5	0.84	0.65	$u_* = 0.3$ m s <sup>-1</sup> four-mode para., mode 2
Lorenz and Murphy [1989]	0.5–1.0	0.43	0.31	$D_p = 0.75$ $\mu\text{m}$
	1.0–2.0	0.78	0.44	$D_p = 1.5$ $\mu\text{m}$
	2.0–5.0	0.92	2.3	$D_p = 3.5$ $\mu\text{m}$
Gallagher et al. [1992]	25–31	–10.9–50.9	31.3	$u_* = 0.3$ m s <sup>-1</sup> $u_* = 0.3$ m s <sup>-1</sup> $z_0 = 1.0$ m four-mode para., mode 4
<i>Urban, <math>z_0 = 5</math> m</i>				
Longley et al. [2004]	0.1–0.2	1.3–3.0	0.4–1.5	$D_p = 0.15$ $\mu\text{m}$
	0.2–0.5	0.1–1.5	0.35–1.4	$D_p = 0.35$ $\mu\text{m}$
	0.5–2.0	0.3–0.8	0.22–1.8	$D_p = 0.8$ $\mu\text{m}$
Freer-Smith et al. [2005]	PM2.5	0.57–5.35	0.5–2.1	$u_* = 0.2$ – $0.6$ m s <sup>-1</sup>
	PM10	0.81–11.0	2.4–34	$u_* = 0.2$ – $0.6$ m s <sup>-1</sup>
	PM100	25.4–36.24	22.5–64.0	
<i>Snow, <math>z_0 = 10^{-3}</math> m</i>				
Duan et al. [1988]	0.15–0.30	0.034	0.029	$D_p = 0.225$ $\mu\text{m}$
	0.5–1.0	0.021	0.020	$D_p = 0.75$ $\mu\text{m}$ $u_* = 0.15$ m s <sup>-1</sup>

observed mean dry deposition velocity smaller than the actual value. Wyers and Duyzer [1997] measured dry deposition velocities of ammonium bisulphate over a coniferous forest, and they obtained a power law relationship  $V_d = 0.0444u_*^{1.47}$ . They suggested that the derived near-linear relationship indicates that a combination of deposition mechanisms is responsible for the dependence of  $u_*$  since a single deposition mechanism of impaction would cause a much stronger dependence of  $u_*$  than a near-linear dependence of  $u_*$ . As shown in Figure 6b and Table 1, in the accumulation mode, if only the impaction mechanism is taken into account, the order of the power law dependence

of  $u_*$  varies from 2.2 to 3.9 for different types of aerosols, with an average of the order being 3.3. Comparisons of the predictions by the four-mode parameterization (mode 2) with these measurements are shown in Figure 8c. The surface roughness length is taken to be 1.5 m. The predictions agree very well with the measurements and the regression of the measurements from very low ( $0.06$  m s<sup>-1</sup>) to very high ( $0.82$  m s<sup>-1</sup>) friction velocities. This very good agreement suggests that the eddy turbulence could be the previously unexplained deposition mechanism.

[36] Characteristics of an urban surface are complicated and it usually has a high roughness length. For comparison,

we take a typical value of 5 m as the urban roughness length, and  $u_*$  in the range of 0.2–0.6 m s<sup>-1</sup>. Longley *et al.* [2004] observed  $V_d$  of 0.3–3.0 cm s<sup>-1</sup> for particles in the aerosol accumulation mode. Correspondingly, the model predicts  $V_d$  in a range of 0.2–1.8 cm s<sup>-1</sup>. Freer-Smith *et al.* [2005] measured  $V_d$  for PM<sub>2.5</sub>, PM<sub>10</sub> and PM<sub>100</sub> in an urban environment, and the ranges of  $V_d$  are 0.6–5.4, 0.8–11.0 and 25.4–36.2 cm s<sup>-1</sup> for each aerosol mode. The four-mode parameterization predicts the ranges of  $V_d$  to be 0.5–2.1, 2.4–34, and 22.5–64.0 cm s<sup>-1</sup>. Considering that the number size distribution of particles, the roughness length and the friction velocity are all assumed, the four-mode parameterization predicts  $V_d$  reasonably well for the urban surface.

[37] A snow surface is usually very smooth and the roughness length is small. From measurements, Duan *et al.* [1988] obtained a mean  $V_d$  of 0.034 and 0.021 cm s<sup>-1</sup> for  $D_p = 0.15$ –0.30 and 0.5–1.0  $\mu\text{m}$  for snow surfaces. For comparison, we take a medium size of the range,  $D_p = 0.225$  and 0.75  $\mu\text{m}$ , respectively. The friction velocity over snow tends to be smaller, and on the basis of the measurement by Duan *et al.*, we take  $u_* = 0.15$  m s<sup>-1</sup>. The model predicts  $V_d = 0.029$  and 0.020 cm s<sup>-1</sup> and agrees very well with the observations.

[38] In a brief summary, we find that the model and the parameterization predict well the measured dry deposition velocities for a wide range of surfaces, from the very smooth snow surface to the very rough urban surface.

## 6. Summary

[39] Traditionally it is believed that, to deposit on the ground surface, an atmospheric aerosol particle passes through a quasi-laminar resistance layer just adjacent to a surface mainly through Brownian diffusion, inertial impaction and gravitational settling. In this study, we introduce a dry deposition mechanism, the burst effect of eddy turbulence, to account for the consistent and systematic underestimation of dry deposition of particles to rough surfaces in some previous process-originated models. A size-solved model is proposed to take into account of each of these mechanisms. Dry deposition by Brownian diffusion is efficient in the nuclei mode and relatively efficient in the accumulation mode, and in this study it is parameterized as a function of the Schmidt number; eddy turbulence (not only the turbulence diffusion, but also the turbulent burst) affects dry deposition in the accumulation mode and the coarse mode, and is parameterized as a function of the roughness Reynolds number. Inertial impaction becomes more and more significant with the increase of particle size in the coarse mode and the giant mode, and is parameterized as a function of the Stokes number (or the dimensionless relaxation time). In the past, it has been noted that the dry deposition velocity is higher for rougher surfaces and more turbulent surface layer winds, but how to physically parameterize these effects on dry deposition is a challenge to modelers. The Sehmel and Hodgson [1978] model is one of a few models that take the surface roughness length into account, but it is mainly a mathematical fitting of the experimental data and lacks a physical meaning of the fitting terms. In this study, we propose a roughness Reynolds term, which accounts for the contribution to dry deposition by turbulence. The effects on the dry deposition

velocity by surface roughness length and friction velocity are described in this term.

[40] Since the dry deposition velocity depends on the particle size significantly, we propose a four-mode parameterization of dry deposition for use in atmospheric dispersion models. The four modes are nuclei mode, accumulation mode, coarse mode and giant mode. For each mode, the mass-averaged dry deposition velocity is calculated. The Brownian and impaction terms of the dry deposition velocity are dependent on the particle diameter, while the turbulence (Reynolds) term is not. After integration over the particle diameter, the bulk dry deposition velocity for each mode is composed of two terms: the Reynolds term and another term which is a function of friction velocity.

[41] The dry deposition velocities predicted by the model and the parameterization are compared with measured dry deposition velocities in the literature and they generally agree well. At the same time, we also note that the model presented in this study is a simplified one. Some other mechanisms or factors affecting dry deposition of atmospheric aerosols, such as thermophoresis, electrostatic forces, and increase of deposition surfaces due to forest canopies, are not included in the model. Under certain conditions, these factors can increase the dry deposition velocity of atmospheric aerosols.

[42] **Acknowledgments.** This study was funded by the Chemical, Biological, Radiological, and Nuclear (CBRN) Research and Technology Initiative (CRTI) of Defence R&D Canada through the CRTI-02-0041RD project. We thank the four anonymous reviewers and the associate editor for their constructive comments. Management support from Richard Hogue and Michel Jean is gratefully acknowledged.

## References

- Allen, A. G., R. M. Harrison, and K. W. Nicholson (1991), Dry deposition of fine aerosol to a short grass surface, *Atmos. Environ., Ser. A*, **25**, 2671–2676.
- Aluko, O., and K. E. Noll (2006), Deposition and suspension of large, airborne particles, *Aerosol Sci. Technol.*, **40**, 503–513, doi:10.1080/02786820600664152.
- Bache, D. H. (1979), Particulate transport within plant canopies (II): Prediction of deposition velocities, *Atmos. Environ.*, **13**, 1681–1687, doi:10.1016/0004-6981(79)90327-5.
- Brutsaert, W. (1982), *Evaporation into the Atmosphere*, D. Reidel, Hingham, Mass.
- Caporali, M., F. Tampieri, F. Trombetti, and O. Vittori (1975), Transfer of particles in nonisotropic air turbulence, *J. Atmos. Sci.*, **32**, 565–568, doi:10.1175/1520-0469(1975)032<0565:TOPINA>2.0.CO;2.
- Davidson, C. I., J. M. Miller, and M. A. Pleskow (1982), The influence of surface structure on predicted particle dry deposition to natural grass canopies, *Water Air Soil Pollut.*, **18**, 25–44, doi:10.1007/BF02419401.
- Doran, J. C., and J. G. Droppo (1983), Profiles of elements in the surface boundary layer, in *Precipitation Scavenging, Dry Deposition and Resuspension*, vol. 2, edited by H. R. Pruppacher, R. G. Semonin, and W. G. N. Slinn, pp. 1003–1012, Elsevier, New York.
- Dorsey, J. R. (2002), Aspects of biosphere atmosphere exchange and chemical processing of aerosol, Ph.D. dissertation, Univ. of Manchester Inst. of Sci. and Technol., Manchester, U. K.
- Duan, B., C. W. Fairall, and D. W. Thomson (1988), Eddy correlation measurements of the dry deposition of particles in wintertime, *J. Appl. Meteorol.*, **27**, 642–652, doi:10.1175/1520-0450(1988)027<0642:ECMOTD>2.0.CO;2.
- Feng, J. (2007), A 3-mode parameterization of below-cloud scavenging of aerosols for use in atmospheric dispersion models, *Atmos. Environ.*, **41**, 6808–6822, doi:10.1016/j.atmosenv.2007.04.046.
- Freer-Smith, P. H., K. P. Beckett, and G. E. Taylor (2005), Deposition velocities to *Sorbus aria*, *Acer campestre*, *Populus deltoides*  $\times$  *trichocarpa* 'Beaupre', *Pinus nigra* and  $\times$  *Cupressocyparis leylandii* for coarse fine and ultra-fine particles in the urban environment, *Environ. Pollut.*, **133**, 157–167, doi:10.1016/j.envpol.2004.03.031.
- Gallagher, M. W., K. Beswick, T. W. Choularton, H. Coe, D. Fowler, and K. Hargreaves (1992), Measurements and modeling of cloudwater de-



- position to moorland and forests, *Environ. Pollut.*, 75, 97–107, doi:10.1016/0269-7491(92)90062-F.
- Gallagher, M., K. Beswick, J. Duyzer, H. Westrate, T. Choularton, and P. Hummelshøj (1997), Measurements of aerosol fluxes to Speulder forest using a micrometeorological technique, *Atmos. Environ.*, 31, 359–373, doi:10.1016/S1352-2310(96)00057-X.
- Gallagher, M. W., E. Nemitz, J. R. Dorsey, D. Fowler, M. A. Sutton, M. Flynn, and J. Duyzer (2002), Measurements and parameterizations of small aerosol deposition velocities to grassland, arable crops, and forest: Influence of surface roughness length on deposition, *J. Geophys. Res.*, 107(D12), 4154, doi:10.1029/2001JD000817.
- Garland, J. A. (1981), *Field Measurements of the Dry Deposition of Small Particles to Grass: Deposition of Atmospheric Pollutants*, edited by H. W. Georgii and J. Pankrath, D. Reidel, Oberursel/Taunus, Germany.
- Giorgi, F. (1986), A particle dry deposition parameterization scheme for use in tracer transport models, *J. Geophys. Res.*, 91, 9794–9804, doi:10.1029/JD091iD09p09794.
- Grönholm, T., P. P. Aalto, V. Hiltunen, Ü. Rannik, J. Rinne, L. Laakso, S. Hyvönen, T. Vesala, and M. Kulmala (2007), Measurements of aerosol particle dry deposition velocity using the relaxed eddy accumulation technique, *Tellus, Ser. B*, 59, 381–386.
- Guha, A. (1997), A unified Eulerian theory of turbulent deposition to smooth and rough surfaces, *J. Aerosol Sci.*, 28, 1517–1537, doi:10.1016/S0021-8502(97)00028-1.
- Hicks, B. B., M. L. Wesely, J. L. Durham, and M. A. Brown (1982), Some direct measurements of atmospheric sulfur fluxes over a pine plantation, *Atmos. Environ.*, 16, 2899–2903, doi:10.1016/0004-6981(82)90040-3.
- Hicks, B. B., M. L. Wesely, R. L. Coulter, R. L. Hart, J. L. Durham, R. E. Speer, and D. H. Stedman (1983), An experimental study of sulfur deposition to grassland, in *Precipitation Scavenging, Dry Deposition and Resuspension*, edited by H. R. Pruppacher, R. G. Semonin, and W. G. N. Slinn, pp. 933–942, Elsevier, New York.
- Hicks, B. B., D. R. Matt, R. T. McMillen, J. D. Womack, M. L. Wesely, R. L. Hart, D. R. Cook, S. E. Lindberg, R. G. de Pena, and D. W. Thomson (1989), A field investigation of sulfate fluxes to a deciduous forest, *J. Geophys. Res.*, 94, 13,003–13,011, doi:10.1029/JD094iD10p13003.
- Horvath, L. (2003), Dry deposition velocity of PM<sub>2.5</sub> ammonium sulfate particles to a Norway spruce forest on the basis of S- and N- balance estimations, *Atmos. Environ.*, 37, 4419–4424, doi:10.1016/S1352-2310(03)00584-3.
- Ibrahim, M., L. A. Barrie, and F. Fanaki (1983), An experimental and theoretical investigation of the dry deposition of particles to snow, pine trees and artificial collectors, *Atmos. Environ.*, 17, 781–788, doi:10.1016/0004-6981(83)90427-4.
- Jaenicke, R. (1993), Tropospheric aerosols, in *Aerosol-Cloud-Climate Interactions*, edited by P. V. Hobbs, pp. 1–31, Academic, San Diego, Calif.
- Kline, S. J., W. C. Reynolds, F. A. Schraub, and P. W. Runstadler (1967), The structure of turbulent boundary layers, *J. Fluid Mech.*, 30, 741–773, doi:10.1017/S0022112067001740.
- Lai, A. C. K., A. B. Miriam, and A. J. H. Goddard (2001), Aerosol deposition in turbulent channel flow on a regular array of three-dimensional roughness elements, *J. Aerosol Sci.*, 32, 121–137, doi:10.1016/S0021-8502(00)00051-3.
- Lamaux, E., A. Labatut, J. Fontan, A. Lopez, A. Druilhet, and Y. Brunet (1994), Biosphere atmosphere exchanges: Ozone and aerosol dry deposition velocities over a pine forest, *Environ. Monit. Assess.*, 31, 175–181, doi:10.1007/BF00547194.
- Legg, B. J., and R. I. Price (1980), The contribution of sedimentation to aerosol deposition to vegetation with a large leaf index, *Atmos. Environ.*, 14, 305–309, doi:10.1016/0004-6981(80)90064-5.
- Liu, B. Y. H., and J. K. Agarwal (1974), Experimental observation of aerosol deposition in turbulent flow, *J. Aerosol Sci.*, 5, 145–155, doi:10.1016/0021-8502(74)90046-9.
- Longley, I. D., M. W. Gallagher, J. D. Dorsey, and M. Flynn (2004), A case-study of fine particle concentrations and fluxes measured in a busy street canyon in Manchester, UK, *Atmos. Environ.*, 38, 3595–3603, doi:10.1016/j.atmosenv.2004.03.040.
- Lorenz, R., and C. E. Murphy Jr. (1989), Dry deposition of particles to a pine plantation, *Boundary Layer Meteorol.*, 46, 355–366, doi:10.1007/BF00172241.
- McRae, G. J., W. R. Goodin, and J. H. Seinfeld (1982), Development of a second-generation mathematical model for urban air pollution, 1. Model formulation, *Atmos. Environ.*, 16, 679–696, doi:10.1016/0004-6981(82)90386-9.
- Muyshondt, A., N. K. Anand, and R. M. McFarland (1996), Turbulent deposition of aerosol particles in large transport tubes, *Aerosol Sci. Technol.*, 24, 107–116, doi:10.1080/02786829608965356.
- Nemitz, E., M. W. Gallagher, J. H. Duyzer, and D. Fowler (2002), Micrometeorological measurements of particle deposition velocities to moorland vegetation, *Q. J. R. Meteorol. Soc.*, 128, 2281–2300, doi:10.1256/qj.0171.
- Nho-Kim, E. Y., M. Michou, and V. H. Peuch (2004), Parameterization of size-dependent particle dry deposition velocities for global modeling, *Atmos. Environ.*, 38, 1933–1942, doi:10.1016/j.atmosenv.2004.01.002.
- Noll, K. E., M. M. Jackson, and A. K. Osisko (2001), Development of an atmospheric particle dry deposition model, *Aerosol Sci. Technol.*, 35, 627–636, doi:10.1080/027868201316899983.
- Owen, P. R. (1969), Pneumatic transport, *J. Fluid Mech.*, 39, 407–432, doi:10.1017/S00222112069002242.
- Peters, K., and R. Eiden (1992), Modeling the dry deposition velocity of aerosol particles to a spruce forest, *Atmos. Environ., Part A*, 26, 2555–2564.
- Pryor, S. C., et al. (2007), A review of measurement and modeling results of particle atmosphere–surface exchange, *Tellus, Ser. B*, 60, 42–75, doi:10.1111/j.1600-0889.2007.00298.x.
- Reeks, M. W. (1983), The transport of discrete particles in inhomogeneous turbulence, *J. Aerosol Sci.*, 14, 729–739, doi:10.1016/0021-8502(83)90055-1.
- Rodean, H. C. (1996), *Stochastic Lagrangian Models of Turbulent Diffusion*, *Meteorol. Monogr.*, vol. 26, 84 pp., Am. Meteorol. Soc., Boston, Mass.
- Ruijgrok, W., C. I. Davidson, and K. W. Nicholson (1995), Dry deposition of particles, *Tellus, Ser. B*, 47, 587–601.
- Ruijgrok, W., H. Tieben, and P. Eisinga (1997), The dry deposition of particles to a forest canopy: A comparison of model and experimental results, *Atmos. Environ.*, 31, 399–415, doi:10.1016/S1352-2310(96)00089-1.
- Schack, C. J., E. P. Sotiris, and S. K. Friedlander (1985), A general correlation for deposition of suspended particles from turbulent gases to completely rough surface, *Atmos. Environ.*, 19, 953–960, doi:10.1016/0004-6981(85)90240-9.
- Sehmel, G. A. (1980), Particle and gas dry deposition: A review, *Atmos. Environ.*, 14, 983–1011, doi:10.1016/0004-6981(80)90031-1.
- Sehmel, G. A., and W. H. Hodgson (1978), A model for predicting dry deposition of particles and gases to environmental surfaces, *DOE Rep. PNL-SA-6721*, Pac. Northwest Lab., Richland, Wash.
- Seinfeld, J. H., and S. N. Pandis (2006), *Atmospheric Chemistry and Physics: From Air Pollution to Climate Change*, John Wiley, Hoboken, N. J.
- Sippola, M. R., and W. W. Nazaroff (2002), Particle deposition from turbulent flow: Review of published research and its applicability to ventilation ducts in commercial buildings, *Rep. LBNL-51432*, Lawrence Berkeley Natl. Lab., Berkeley, Calif.
- Slinn, W. G. N. (1982), Predictions of particle deposition to vegetative surfaces, *Atmos. Environ.*, 16, 1785–1794, doi:10.1016/0004-6981(82)90271-2.
- Slinn, S. A., and W. G. N. Slinn (1980), Predictions for particle deposition on natural waters, *Atmos. Environ.*, 14, 1013–1026, doi:10.1016/0004-6981(80)90032-3.
- Van Aalst, R. M. (1986), Dry deposition of aerosol particles, in *Aerosols*, edited by S. D. Lee et al., pp. 933–949, Lewis, Chelsea, Mich.
- Vong, R. J., D. Vickers, and D. S. Covert (2004), Eddy correlation measurements of aerosol deposition to grass, *Tellus, Ser. B*, 56, 105–117.
- Webb, R. L. (1979), Toward a common understanding of the performance and selection of roughness for forced convection, in *Studies in Heat Transfer: A Festschrift for E. R. G. Eckert*, edited by J. P. Hartnett et al., Hemisphere, Washington, D. C.
- Wesely, M. L., and B. B. Hicks (2000), A review of the current status of knowledge on dry deposition, *Atmos. Environ.*, 34, 2261–2282, doi:10.1016/S1352-2310(99)00467-7.
- Wesely, M. L., D. R. Cook, R. L. Hart, and R. E. Speer (1985), Measurements and parameterization of particle sulfur deposition over grass, *J. Geophys. Res.*, 90, 2131–2143, doi:10.1029/JD090iD01p02131.
- Williams, R. M. (1982), A model for the dry deposition of particles to natural water surfaces, *Atmos. Environ.*, 16, 1933–1938, doi:10.1016/0004-6981(82)90464-4.
- Wiman, B. L. B., and G. I. Agren (1985), Aerosol depletion and deposition in forests, a model analysis, *Atmos. Environ.*, 19, 335–362, doi:10.1016/0004-6981(85)90101-5.
- Wyers, G. P., and J. H. Duyzer (1997), Micrometeorological measurement of the dry deposition flux of sulphate and nitrate aerosols to coniferous forest, *Atmos. Environ.*, 31, 333–343, doi:10.1016/S1352-2310(96)00188-4.
- Young, J., and A. Leeming (1997), A theory of particle deposition in turbulent pipe flow, *J. Fluid Mech.*, 340, 129–159, doi:10.1017/S0022112097005284.
- Zhang, L., S. Gong, J. Padro, and L. Barrie (2001), A size-segregated particle dry deposition scheme for an atmospheric aerosol module, *Atmos. Environ.*, 35, 549–560, doi:10.1016/S1352-2310(00)00326-5.

J. Feng, Canadian Meteorological Centre, Meteorological Service of Canada, 2121 Trans-Canada Highway, Dorval, QC, Canada, H9P 1J3. (jian.feng@eg.gc.ca)